Journal of
Nanoscience and Nanotechnology
Vol. 13, 3645–3649, 2013

Improved Photoluminescence Efficiency in UV Nanopillar Light Emitting Diode Structures by Recovery of Dry Etching Damage

Dae-Woo Jeon[1,2], Lee-Woon Jang[1], Ju-Won Jeon[1], Jae-Woo Park[1], Young Ho Song[2], Seong-Ran Jeon[2], Jin-Woo Ju[2], Jong Hyeob Baek[2], and In-Hwan Lee[1,*]

[1] *School of Advanced Materials Engineering and Research Center of Advanced Materials Development, Chonbuk National University, Jeonju 561-756, Korea*
[2] *LED Research Division, Korea Photonics Technology Institute, Gwangju 500-779, Korea*

In this study, we have fabricated 375-nm-wavelength InGaN/AlInGaN nanopillar light emitting diodes (LED) structures on *c*-plane sapphire. A uniform and highly vertical nanopillar structure was fabricated using self-organized Ni/SiO_2 nano-size mask by dry etching method. To minimize the dry etching damage, the samples were subjected to high temperature annealing with subsequent chemical passivation in KOH solution. Prior to annealing and passivation the UV nanopillar LEDs showed the photoluminescence (PL) efficiency about 2.5 times higher than conventional UV LED structures which is attributed to better light extraction efficiency and possibly some improvement of internal quantum efficiency due to partially relieved strain. Annealing alone further increased the PL efficiency by about 4.5 times compared to the conventional UV LEDs, while KOH passivation led to the overall PL efficiency improvement by more than 7 times. Combined results of Raman spectroscopy and X-ray photoelectron spectroscopy (XPS) suggest that annealing decreases the number of lattice defects and relieves the strain in the surface region of the nanopillars whereas KOH treatment removes the surface oxide from nanopillar surface.

Keywords: InGaN/AlInGaN LED, Nanopillar, Dry Etching, Chemical Treatment.

RESEARCH ARTICLE

1. INTRODUCTION

Group III nitride-based ultraviolet (UV) light emitting diodes have attracted great attention because of their potential to replace conventional mercury-containing lamps for some applications including UV sensing, curing and photo-catalysis.[1,2] Also, the UV LEDs can be used as a pumping source for developing the white-light LEDs to solve the problem of low color-rending index by conventional white-light LEDs.[3,4]

At the same time, due to the great advantages of the nanostructures over the bulk material, these nanostructures have been widely tested in many useful device applications such as super-bright LEDs, full color displays, etc.[5]

Among the advantages of nanostructures one should name their ability to relieve the strain caused by the lattice mismatch at hetero-interfaces, thus enhancing the internal quantum efficiency of LED devices.[6] Also, due to a large sidewall surface area of nanopillars, light extraction efficiency can be greatly improved.[5,7] In addition, in selectively grown nanostructures, inclined threading dislocations can be effectively terminated at the nanopillar sidewalls, thus decreasing the dislocation density (although this effect is not expected to occur in nanostructures prepared by selective etching).[8]

For GaN-based nanoscale structures, the GaN nanopillars have been produced by various fabrication methods, such as growth of InGaN/GaN multiple quantum nanocolumns/nanopillars on Si substrate by radio-frequency plasma-assisted molecular-beam epitaxy[9] or growth of single-crystal GaN nanopillars by hybrid vapor-phase epitaxy,[10] synthesis of GaN nanocolumns using carbon nanotubes as templates,[11] producing of nanopillar arrays by inductively coupled plasma-reactive ion etching (ICP-RIE) without masks[12] or by *e*-beam patterning.[13] Each of these approaches is technologically quite challenging. To simplify the patterning process, it is possible to produce nanoscale self-assembled nickel (Ni) dots

*Author to whom correspondence should be addressed.

serving as an etching mask on top of the LED surface by choosing the correct Ni layer thickness, annealing time and annealing temperature.[14]

However, nanopillars made by top–down process can be easily contaminated or damaged during the etching processes,[15] resulting in poor optical properties. Recently, Zhu et al. have reported on etching damage of nanopillar LEDs fabricated by using Ni dots and demonstrated enhancement of photoluminescence (PL) intensity after KOH treatment.[8] Unfortunately, the cause of the PL intensity improvement due to the chemical treatment was not clearly understood. Also, nanopillar structures out of InGaN/AlInGaN based UV LED have not been so far explored.

In this letter, we describe the fabrication of the UV InGaN/AlInGaN nanopillar LED structures by using self-assembled Ni dots. The effects of thermal annealing and surface treatment of as-fabricated nanopillars on their PL efficiency was investigated in detail. It was demonstrated that the combination of these two treatments allows to strongly suppress the detrimental influence of damage produced by dry etching.

2. EXPERIMENTAL DETAILS

The UV InGaN/AlInGaN LED was grown by MOCVD on a *c*-axis sapphire (0001) substrate. Five $In_{0.04}Ga_{0.96}N$/$Al_{0.08}In_{0.01}Ga_{0.91}N$ quantum wells (QWs) were sandwiched between Si-doped thick *n*-GaN layer and 200 nm thick Mg-doped *p*-GaN top cladding layer.

The UV LED nanopillar structure fabrication process is illustrated by Figure 1. The first step was a 100 nm SiO_2 interlayer deposition on top of the LED samples by a plasma-enhanced chemical vapor deposition (PECVD) technique. After the SiO_2 deposition, a 10 nm Ni layer was deposited on SiO_2 interlayer by *e*-beam evaporation. The Ni on SiO_2 interlayer LED samples were subsequently subjected to rapid temperature annealing (RTA) under flowing N_2 at 850 °C for 1 min to form self-assembled Ni metal clusters. ICP etching was conducted to etch the exposed SiO_2 film using the Ni nano dots as an etch mask. The etching gas used was a mixture of the O_2 and CF_4. Then the MQW structure was further etched down to the *n*-type GaN layer by the ICP etching with gas of Cl_2. Finally, the Ni/SiO_2 was removed by a buffered oxide etchant to expose the InGaN/AlInGaN MQW nanopillars.

The samples were then divided into two batches and subjected to different treatments. Firstly, the samples were annealed in flowing N_2 at 900 °C by RTA (rapid thermal annealing). Secondly, the fabricated nanopillars were treated in KOH 0.1 mol (KOH:H_2O) for 45 sec.

The morphology and shape of nanopillars was analyzed by field emission scanning electron microscope (FE-SEM). The X-ray photoelectron spectroscopy (XPS) was employed to examine the change of surface characteristics caused by the chemical treatment. The PL spectra

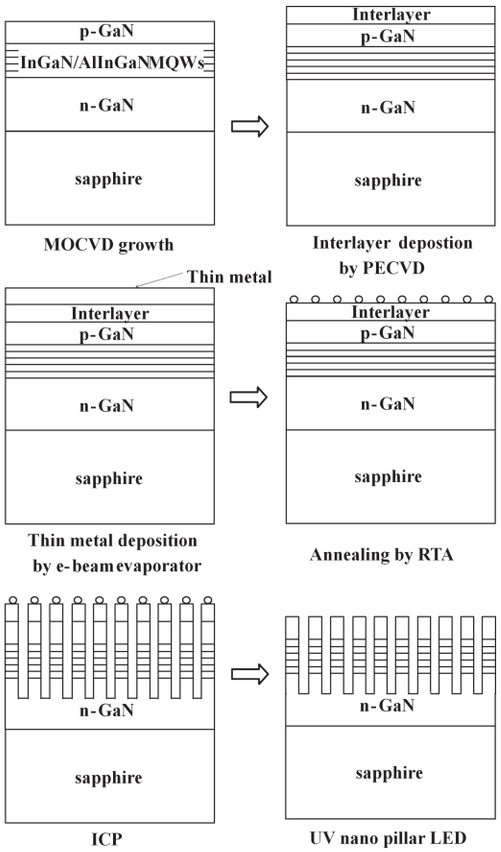

Fig. 1. Schematic diagram for the fabrication of UV nanopillar LED.

measurements were carried out to study the optical properties at each stage. In these measurements, a He–Cd laser (325 nm) was used for excitation with power densities up to 10 W/cm^2. The Raman spectroscopy measurements were carried out at room temperature using the 514 nm line of an Ar^+ laser as an excitation source.

3. RESULTS AND DISCUSSION

Figure 2(a) shows the FE-SEM image of Ni nanodot arrays formed on SiO_2/LED structure after the RTA process. The SiO_2 layer between the thin Ni layer and the

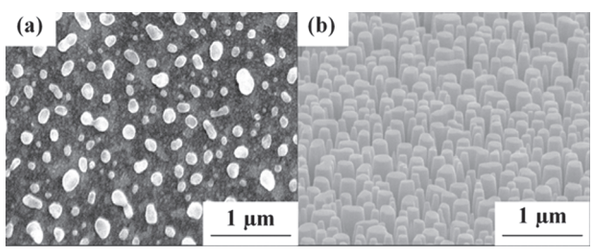

Fig. 2. (a) FE-SEM images of Ni nanodot arrays formed on SiO_2/LED and (b) UV nanopillar arrays with nanopillar diameter of 150–200 nm and length of ~500 nm.

RESEARCH ARTICLE

LED surface helps to form highly dense and spherical Ni nanodots by offering dewetting conditions for Ni film during the annealing process. This is because, in contrast to the top GaN layer providing good wetting conditions for the metal due to the high surface energy, the SiO_2 layer is a stable oxidized substance that has a low surface energy. Its lower surface energy provides better conditions for the formation of a high density of metal droplets. With the Ni nanodots/SiO_2 on the planar LED template, the ICP etching was done to fabricate the vertical and highly dense nanopillar LED arrays. Figure 2(b) shows SEM image of UV nanopillar arrays with nanopillar diameter of 150–200 nm and length of $\sim$500 nm. The nanopillar size was controllable by the Ni layer thickness, the annealing time and temperature and the ICP etching time.

During the fabrication of nanopillars, the sidewall of nanopillar can experience serious surface damage from the low-energy ions in ICP process plasma.[16] Energetic ion bombardment can create lattice defects, lead to the formation of dangling bonds on the surface, or to the incorporation of the ions from the ICP plasma ambience into the surface via ion implantation. These defects often act as deep level states and produce compensation, trapping, or recombination sites in the material.[17] In order to take full advantage of nanopillar LED approach, it is essential to develop appropriate post-plasma etching treatments to remove plasma damage generated in the nanopillar sidewalls. Below it is shown that high temperature annealing in inert atmosphere followed by surface chemical treatment in KOH solution can be very effective means to achieve that goal.

Figure 3 shows the room temperature PL spectra taken for conventional planar UV LED, UV nanopillar LED, annealed UV nanopillar LED, and annealed UV nanopillar LED with chemical treatment. As can be seen, the PL intensity of the nanopillar LED is more than two times higher than that of conventional LED. The corresponding PL peak energies were 3.311 and 3.298 eV, respectively. As Zhu et al. previously discussed,[7] the increased PL intensity is attributable to the light scattering at the sidewalls of nanopillars and the increased overlap of the electron and the hole wavefunctions. Indeed, the sidewalls of the nanopillar play an important role in extracting light efficiently. A larger surface area is desirable since it provides more pathways by which generated photons can escape.[18–20] In strained nitride QWs, the piezoelectric field decreases the overlap of the electron and the hole wavefunctions (i.e., the field tilts the energy bands of MQWs), and reduces internal quantum efficiency. This compressive strain in the MQWs can be effectively relieved in nanopillar structures, resulting in the enhanced PL yield. We note that the PL energy difference (EPL) is a measure of strain built in the MQWs. In this work using UV MQW structure, the lattice mismatch between $In_{0.04}Ga_{0.96}N$ well and $Al_{0.08}In_{0.01}Ga_{0.91}N$ barrier was 0.6%, and the corresponding EPL was 13 meV. On the other hand, in our previous study using a blue LED structure,[20] the lattice mismatch between InGaN well and GaN barrier was 2.5%, and the EPL was 64 meV. The full width at half maximum (FWHM) of the PL peak is decreased from 119 meV for the conventional UV LED to 96 meV for the UV nanopillar LED (see Fig. 3). As the tilted energy band broadens PL spectrum, the decreased PL linewidth for nanopillar structure is an additive evidence of the strain reduction in the MQWs.

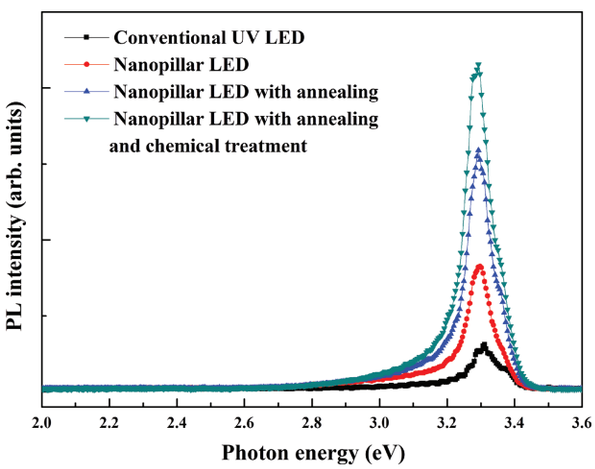

Fig. 3. PL spectra at room temperature for conventional UV LED, UV nanopillar LED, and treated UV nanopillar LEDs.

As seen from Figure 3 high temperature annealing leads to further increase of PL intensity compared to the conventional UV LED structure. We attribute this improvement to annealing of the dry-etching-induced near-surface defects that act as nonradiative recombination centers. The indirect confirmation is provided by the observed decrease in strain after annealing, as evidenced by Raman spectra measurements performed on as-etched and etched and annealed samples. We were tracking the position of the E_2 (high) mode known to be sensitive to strain, but not to electron concentration.[21] The E_2 (high) line frequency has been reported to shift towards the higher frequency region with increasing compressive strain at the rate of 2.9 cm^{-1}/GPa.[21]

Figure 4 shows Raman spectra taken for the spectral region near the E_2 (high) line for the conventional UV LED (568.5 cm^{-1}), the UV nanopillar LED (568.2 cm^{-1}) and annealed UV nanopillar LED (567.9 cm^{-1}), respectively. A quite measurable lower frequency shift can be clearly observed after annealing and the E_2 (high) frequency of the annealed sample is very close to the frequency of free-standing GaN that is presumably strain-free.[22, 23] We attribute this strain relaxation after annealing to annihilation of defects produced at the surface of GaN by plasma etching.

KOH etching after annealing leads to a further increase of PL intensity, as shown in Figure 3. To better understand

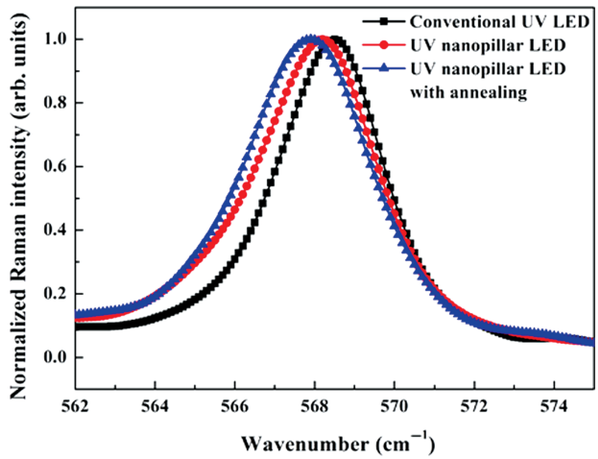

Fig. 4. Raman spectra for the spectral region near the E_2 (high) line for the conventional UV LED, UV nanopillar LED and annealed UV nanopillar LED.

the nature of the effect, we performed XPS measurements on the annealed and chemically treated UV nanopillar samples. The results are compared in Figure 5. An oxygen related peak near 531 eV for photoelectrons due to transition from the O 1s state[24] could be clearly seen in the as-etched sample suggesting the formation of a native oxide layer after etching which is not totally unexpected given the etching ambience. Chemical treatment in KOH solution obviously greatly decreases the oxygen related XPS signal manifesting effective removal of the oxide layer that is most likely the native oxide GaO_x known to have been effectively removed by KOH treatment.[25]

Concomitant increase in PL intensity could then be due to corresponding removal of the surface band bending at the nanopilar sidewall. The effect of KOH treatment is similar to the previously reported effect of HCl treatment[8] and it could be suggested that the nature of the observed PL increase is similar in both cases.

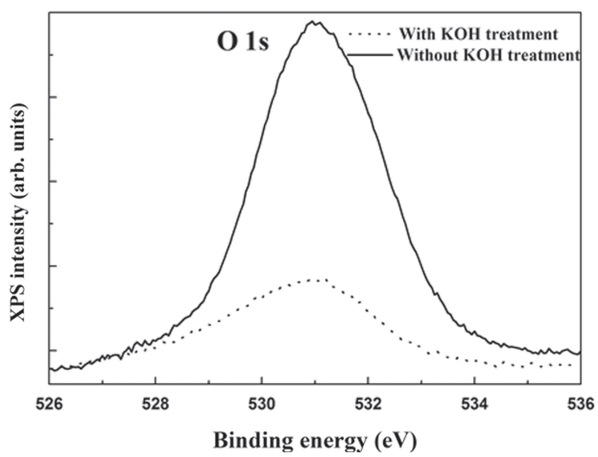

Fig. 5. XPS spectra for the UV nanopillar LED with KOH treatments.

4. CONCLUSION

In this study, we have fabricated 375 nm wavelength InGaN/AlInGaN nanopillars light emitting diode (LED) structures on *c*-plane sapphire. The UV nanopillar LED structure was fabricated by using self-assembled Ni nano mask. The height and diameter of nanopillars in these UV LED structures were 500 nm and 150 nm, respectively. The PL intensity of these as-etched nanopillar structures was more than two times higher than for the conventional UV LED structures, most likely due to increased light extraction efficiency. The relaxation of residual strain of the as-etched UV nanopillar LED structure could be achieved by high temperature annealing and was accompanied by substantial PL intensity increase due to annealing of the surface damage defects produced by dry etching. Additional KOH treatment after annealing led to further increase of PL intensity (the PL intensity increase after this two-stage treatment was by more than 7 times compared to the standard structure). This PL intensity increase is attributed to the removal of the native oxide layer formed during dry etching, as evidenced by XPS measurements.

Acknowledgment: This work was supported by the National Research Foundation of Korea (NRF) funded by the Korea government (MEST) (2010-0019626, 2010-0026614).

References and Notes

1. J. C. Zhang, Y. H. Zhu, T. Egawa, S. Sumiya, M. Miyoshi, and M. Tanaka, *Appl. Phys. Lett.* 92, 191917 (**2008**).
2. V. Adivarahan, A. Chitnis, J. P. Zhang, M. Shatalov, J. W. Yang, G. Simin, M. Asif Khan, R. Gaska, and M. S. Shur, *Appl. Phys. Lett.* 79, 4240 (**2001**).
3. H. Hirayama, A. Kinoshita, T. Yamabi, Y. Enomoto, A. Hirata, T. Araki, Y. Nanishi, and Y. Aoyagi, *Appl. Phys. Lett.* 80, 207 (**2002**).
4. C. Chen, J. Yang, M. Y. Ryu, J. Zhang, E. Kuokstis, G. Simin, M. Asif Khan, *Jpn. J. Appl. Phys.* 41, 1924 (**2002**).
5. H. M. Kim, Y. H. Cho, H. Lee, S. I. Kim, S. R. Ryu, D. Y. Kim, T. W. Kang, and K. S. Chung, *Nano Lett.* 6, 1059 (**2004**).
6. C. J. Neufeld, C. Schaake, M. Grundmann, N. A. Fichtenbaum, S. Keller, and U. K. Mishra, *Phys. Stat. Sol.* (*c*) 4, 1605 (**2007**).
7. J. H. Zhu, L. Wang, S. Zhang, H. Wang, D. Zhao, J. J. Zhu, Z. Liu, D. Jiang, and H. Yang, *J. Appl. Phys.* 108, 074302 (**2010**).
8. J. H. Zhu, S. M. Zhang, X. Sun, D. G. Zhao, J. J. Zhu, Z. S. Liu, D. S. Jiang, L. H. Duan, H. Wang, Y. S. Shi, S. Y. Liu, and H. Yang, *Chin. Phys. Lett.* 25, 3485 (**2008**).
9. A. Kikuchi, M. Kawai, M. Tada, and K. Kishino, *Jpn. J. Appl. Phys.* 43, L1524 (**2004**).
10. H. M. Kim, D. S. Kim, T. W. Kang, Y. H. Cho, and K. S. Chung, *Appl. Phys. Lett.* 84, 2193 (**2002**).
11. W. Q. Han, S. S. Fan, Q. Q. Li, and Y. D. Hu, *Science* 277, 1287 (**1997**).
12. C. C. Yu, C. F. Chu, J. Y. Tsai, H. W. Huang, T. H. Hsueh, C. F. Lin, and S. C. Wang, *Jpn. J. Appl. Phys.* 41, L910 (**2002**).
13. H. S. Chen, D. M. Yeh, Y. C. Lu, C. Y. Chen, C. F. Huang, T. Y. Tang, C. C. Yang, C. S. Wu, and C. D. Chen, *Nanotechnology* 17, 1454 (**2006**).
14. J. D. Carey, L. L. Ong, and S. R. P. Silva, *Nanotechnology* 14, 1223 (**2003**).
15. H. Yagi, K. Muranushi, N. Nunoya, T. Sano, S. Tamura, and S. Arai, *Appl. Phys. Lett.* 81, 966 (**2002**).

RESEARCH ARTICLE

16. Y. B. Hahn, R. J. Choi, J. H. Hong, H. J. Park, C. S. Choi, and H. J. Lee, *J. Appl. Phys.* 92, 1189 **(2002)**.
17. H. S. Yang, S. Y. Han, K. H. Baik, and S. J. Pearton, *Appl. Phys. Lett.* 86, 102104 **(2005)**.
18. M. Yamada, T. Mitani, Y. Narukawa, S. Shioji, I. Niki, S. Sonobe, K. Deguchi, M. Sano, and T. Mukai, *Jpn. J. Appl. Phys.* 41, 1431 **(2002)**.
19. Y. L. Lai, C. P. Liu, Y. H. Lin, R. M. Lin, D. Y. Lyu, Z. X. Peng, and T. Y. Lin, *Appl. Phys. Lett.* 89, 151906 **(2006)**.
20. D. W. Jeon, W. M. Choi, H. J. Shin, S. M. Yoon, J. Y. Choi, L. W. Jang, and I. H. Lee, *J. Mater. Chem.* 21, 17688 **(2011)**.
21. T. Inoue, Y. Toda, K. Hoshino, T. Someya, and Y. Arakawa, *Phys. Stat. Sol. (c)* 7, 2428 **(2003)**.
22. C. Kisielowski, J. Kruger, S. Ruvimov, T. Suski, J. W. Ager, III, E. Jones, Z. Liliental-Weber, M. Rubin, and E. R. Weber, *Phys. Rev. B* 54, 24 **(1996)**.
23. H. W. Seo, Q. Y. Chen, M. N. Iliev, L .W. Tu, C. L. Hsiao, James K. Mean, W.-K. Chu, *Appl. Phys. Lett.* 88, 153124 **(2006)**.
24. K. Kotsis and V. Staemmler, *Phys. Chem. Chem. Phys.* 8, 1490 **(2006)**.
25. J. L. Lee, J. K. Kim, J. W. Lee, Y. J. Park, and T. Kim, *Solid-State Electronics* 43, 435 **(1999)**.

Received: 24 January 2011. Accepted: 9 June 2012.